NPL

NPL REPORT MAT 53

A Heat Transport Model for Multiphase Materials

Simon Roberts, Jim Robinson, Keith Lawrence

JANUARY 2012

A Heat Transport Model for Multiphase Materials

Simon Roberts, Jim Robinson, Keith Lawrence
Materials Division

ABSTRACT

A model is presented that can be used to predict thermal transport through a material taking into account any changes of material phase. A finite volume modelling approach is described that uses conservation of energy to balance the heat fluxes into a volume element. The finite volume model may be applied to three-dimensional, multi-material systems subjected to applied temperature and heat flux boundary conditions. The mathematical derivations in this report do not include explicit expressions describing the change in thermal properties with temperature and phase, however a method is described using a modified energy balance to link with the thermodynamic phase equilibria package MTDATA.

The linking of the NPL thermal transport model TherMOL 3D with MTDATA to form a hybrid model is described, providing a relationship between temperature and stored energy. Predictions from the TherMOL 3D software and the hybrid TherMOL 3D/MTDATA software are presented, which show temperature curves for a steel slab subjected to heat flux boundary conditions held constant in time. These predictions clearly show the difference in temperature upon heating between the TherMOL 3D software and hybrid software due to corrections for phase changes. Analyses of grid sizes are shown to have a significant effect on cell temperatures due to neighbouring cell phase changes.

ISSN 1754-2979

National Physical Laboratory
Hampton Road, Teddington, Middlesex, TW11 0LW

Approved on behalf of NPLML by Markys Cain, Materials Knowledge Leader.

CONTENTS

1 INTRODUCTION

The rate at which heat is transferred through a material is of great importance to engineers and manufacturers. Depending on the application it may be desirable to have a slow transfer of heat, for insulating purposes, or a fast transfer of heat, for increased productivity in moulding applications or for higher efficiency heat exchangers (Armitt *et al* 1978). Thermal conductivity data is of prime importance when designing heat exchangers as heat transfer coefficients in these components are usually computed using correlations that depend on thermal conductivity. In industrial processes, where there are demanding high temperature environments, phase changes can significantly affect the material properties and performance of the final components (Chapman 2004).

To understand better how a material is thermally performing under service conditions or during manufacturing it is desirable to use modelling and visualisation techniques to predict the material response. For example, the first version of the NPL developed software TherMOL solved the two-dimensional heat-conduction equation using control volume finite differences and combined this approach with inverse modelling techniques to predict successfully the thermal properties of layered materials from laser flash temperature data (Chapman *et al* 2005). In the aerospace industry, modelling is necessary in the design and optimisation of the lifetime of components such as turbine blades (Howse 2004).

The basic theory for the mathematics of heat transfer is described in detail by Lienhard 2004 and Incropera and DeWitt 1981. There have been many analytical approaches for solving the heat transfer equation, in particular, Carslaw and Jaeger 1993 give extensive derivations of mostly analytical solutions to heat transfer problems by obtaining solutions for simple geometries using various boundary conditions. Most of these standard approaches use Fourier's law (Fourier 1822), which is applicable to most materials systems where the thermal conduction and other thermal properties are fixed. In materials systems where the thermal properties are changing due to changes in temperature, phase etc alternative approaches are required. There have been analytical solutions generalising properties such as thermal conductivity (Feng *et al* 2004) and in non-equilibrium thermodynamics there have been methods developed to include non-equilibrium variables (such as heat flux) in the entropy (Jou and Casas-Vazquez 1988). However, for materials with complex geometries and numerous components a numerical approach is needed.

In this report, the three-dimensional heat-conduction equation for a homogeneous material is derived by applying the principle of conservation of energy through a control volume. This basic theory is extended to apply to three-dimensional multi-material systems composed of adjacent homogeneous blocks. Energy balances are constructed for each block or volume so that finite volume equations can be derived for each discrete volume. The finite volume equations are solved numerically using an explicit method to determine the temperature distribution at a series of incremental discrete time steps. The derivation of the finite volume equations in this report follows a similar approach for mass diffusion by Duncan *et al* 2007 and is the basis for the NPL software package TherMOL 3D.

The mathematical derivations outlined in this report are written in a form where there are no explicit equations that describe the change in thermal properties with temperature and material phase. The finite volume energy balance is modified so a term representing the rate of change of internal energy is used as a mechanism for a thermodynamic model to be implemented into the thermal transport equations. Using this theory, MTDATA (Davies *et al* 2002), the thermodynamic and phase equilibria software package developed at NPL, has been linked into TherMOL 3D at a fundamental level in order to provide the relationship between the stored energy and the temperature of a cell. The linked TherMOL 3D/MTDATA model will be referred to as the *hybrid model* for the rest of this report. The hybrid model is able to determine the transient thermal distribution of three-dimensional multi-material systems where changes in thermal properties, resulting from changes in material phase and temperature, are taken fully into account.

2 FINITE VOLUME EQUATIONS FOR THREE-DIMENSIONAL TRANSIENT HEAT DIFFUSION

Although there exist many analytical solutions to the heat diffusion equation with various boundary conditions, multi-layered or multi-material structures have to be solved using numerical methods. For determining heat transfer in systems where the geometry is generally static the most suitable approach is to use finite difference or finite volume methods (Peiró and Sherwin 2005).

Both Incropera and DeWitt and Carslaw and Jaeger have substantial sections on solving heat transfer problems using finite difference numerical methods. The finite difference method is a Taylor series approach that divides the continuum into nodes. The underlying partial differential equation is then approximated node wise using finite differences, which is simple and straightforward for orthogonal grids with simple boundary conditions. In this report, solutions of the heat transfer equation are derived using the more popular finite volume approach described by Barth and Ohlberger 2004. This is based on the physical concept of using macroscopic control volumes to numerically solve the conservation laws of heat transfer. In the finite volume method, the integration domain is covered by control volumes (cells) where each volume engulfs one node that lies on a grid. The discretisation equations are obtained by integrating over the control volumes surrounding the nodes, after introducing necessary simplifications and assumptions. This often leads to the same discretisation equations as the Taylor series method, however it is much more flexible and has much in common with the Galerkin finite element method (Hsu 1986) but is easier to implement. The basic equations are now derived for modelling the transient heat transfer through a three-dimensional homogeneous material, subjected to fixed temperature and heat flux boundary conditions.

2.1 INTEGRAL FORM OF THE ENERGY EQUATION

The law of conservation of energy states that the total amount of energy in an isolated system is conserved over time. For a given volume within the system, energy may enter or leave due to transport across the surface or be generated within the volume (for example from chemical reactions). Neglecting any source terms, the well-known rate equation describing the conservation of energy (Hong 2004) is

$$\frac{\partial}{\partial t}\left(\rho c_v T\right) = -\nabla.\mathbf{q}\,, \tag{2.1}$$

where T is the temperature, **q** is the heat flux vector, ρ is the density and c_v is the specific heat at constant volume. Now consider a region V bounded by a closed surface S across which heat may flow. Integrating (2.1) over the region leads to

$$\int_V \frac{\partial}{\partial t}\left(\rho c_v T\right) dV = -\int_V \nabla.\mathbf{q}\, dV\,. \tag{2.2}$$

Applying the divergence theorem to (2.2) yields

$$\int_V \frac{\partial}{\partial t}\left(\rho c_v T\right) dV = -\int_S \mathbf{n}.\mathbf{q}\, dS\,, \tag{2.3}$$

where **n** is the outward unit normal to the surface S bounding the region V. The relation (2.3) is the integral form of the energy balance equation and defines the relationship between rate of change of temperature within the volume and the temperature flux across the boundary. We now consider a control volume in the form of a rectangular parallelepiped whose sides are parallel to the Cartesian

coordinate axes x, y and z and are of lengths Δx, Δy and Δz respectively, such that the volume of the cell is simply

$$\Delta V = \Delta x.\Delta y.\Delta z\,. \tag{2.4}$$

If we assume that the cell size is small enough for the rate change of temperature, density and specific heat to be regarded as uniform throughout the control volume, then the left hand side of (2.3) may be written

$$\int_V \frac{\partial}{\partial t}(\rho c_v T)\,dV = \int_z^{z+\Delta z}\int_y^{y+\Delta y}\int_x^{x+\Delta x} \frac{\partial}{\partial t}(\rho c_v T)\,dx\,dy\,dz = \frac{\partial}{\partial t}(\rho c_v T)\Delta x\,\Delta y\,\Delta z\,. \tag{2.5}$$

The surface integral in (2.3), when applied to the control volume, can be written

$$\begin{aligned} -\int_S \mathbf{n}.\mathbf{q}\,dS = {} & \int_z^{z+\Delta z}\int_y^{y+\Delta y}(q_x - q_{x+\Delta x})\,dy\,dz + \\ & \int_z^{z+\Delta z}\int_x^{x+\Delta x}(q_y - q_{y+\Delta y})\,dx\,dz + \\ & \int_y^{y+\Delta z}\int_x^{x+\Delta y}(q_z - q_{z+\Delta z})\,dx\,dy\,, \end{aligned} \tag{2.6}$$

where q is a scalar term describing the components, indicated by respective subscripts, of the heat flux vectors across the boundaries at x, y, z, x+Δx, y+Δy and z+Δz. Assuming the flux components are uniform across each boundary of the control volume, the integration of (2.6) yields

$$-\int_S \mathbf{n}.\mathbf{q}\,dS = (q_x - q_{x+\Delta x})\Delta y\,\Delta z + (q_y - q_{y+\Delta y})\Delta x\,\Delta z + (q_z - q_{z+\Delta z})\Delta x\,\Delta y\,. \tag{2.7}$$

It is sufficient in most applications of heat conducting through solids to use Fourier's law, which defines, for any point within the system, the flux vector as

$$\mathbf{q} = -\lambda\,\nabla T\,, \tag{2.8}$$

where λ is the thermal conductivity coefficient that usually depends upon the temperature T. This form assumes that there are no temperature or stress gradients in the system. The use of (2.8) is thus an approximation for many practical applications. Using (2.8), equation (2.7) can be rewritten as

$$\begin{aligned} -\int_S \mathbf{n}.\mathbf{q}\,dS = {} & \left(\lambda_{x+\Delta x}\left.\frac{\partial T}{\partial x}\right|_{x+\Delta x} - \lambda_x\left.\frac{\partial T}{\partial x}\right|_x\right)\Delta y\,\Delta z + \\ & \left(\lambda_{y+\Delta y}\left.\frac{\partial T}{\partial y}\right|_{y+\Delta y} - \lambda_y\left.\frac{\partial T}{\partial y}\right|_y\right)\Delta x\,\Delta z + \\ & \left(\lambda_{z+\Delta z}\left.\frac{\partial T}{\partial z}\right|_{z+\Delta z} - \lambda_z\left.\frac{\partial T}{\partial z}\right|_z\right)\Delta x\,\Delta y\,, \end{aligned} \tag{2.9}$$

where the subscripts x, y, z, x+Δx, y+Δy and z+Δz refer to the values of the thermal conductivities and derivatives at the respective control volume boundaries.

2.2 FINITE VOLUME REPRESENTATION OF THE CONSERVATION OF ENERGY

Any multi-material structure can be described approximately by a collection of discrete cells, where each cell represents a homogeneous material block. A simple orthogonal grid is constructed where each node represents the centre of each cell as shown in Figure 2.1. The finite volume equations are obtained by integrating (2.1), over the cell volume surrounding each grid node, for a discrete time interval. For each time interval it is assumed that the temperatures internally and at the boundary are fixed.

We take this opportunity to introduce the notation to be used in this report. From here on, a variable associated with the $(i,j,k)^{th}$ node will have the subscript (i,j,k). For example, the temperature *at* the $(i,j,k)^{th}$ node would be denoted by $T_{(i,j,k)}$. Similarly values of other parameters associated with the $(i,j,k)^{th}$ node would also have the (i,j,k) subscript, for example the size of the $(i,j,k)^{th}$ cell in the x-direction would be notated as $\Delta x_{(i,j,k)}$. The notation is extended to the heat fluxes *across* the cell boundaries. The symbols $\rightarrow$, $\uparrow$, $\bullet$ indicate the values of fluxes in the positive x, y and z directions respectively. The symbols $\leftarrow$, $\downarrow$, $\otimes$ will be used to indicate the values of fluxes in the negative x, y and z directions respectively. For example, the flux at the interface between the $(i-1,j,k)^{th}$ node and the $(i,j,k)^{th}$ node, in the direction *towards* the $(i,j,k)^{th}$ node (in the positive x-direction) would be $q_{(i-1,j,k)\rightarrow(i,j,k)}$. Finally, the superscripts p and p+1, where p = 0, 1, 2, …., will represent the values of the state variables at the p^{th} and $p+1^{th}$ time steps when the time has values t_p and t_{p+1} respectively, where the size of each time step is denoted by $\Delta t_{P+1} = t_{P+1} - t_p$, and where it is assumed that $t_0 = 0$.

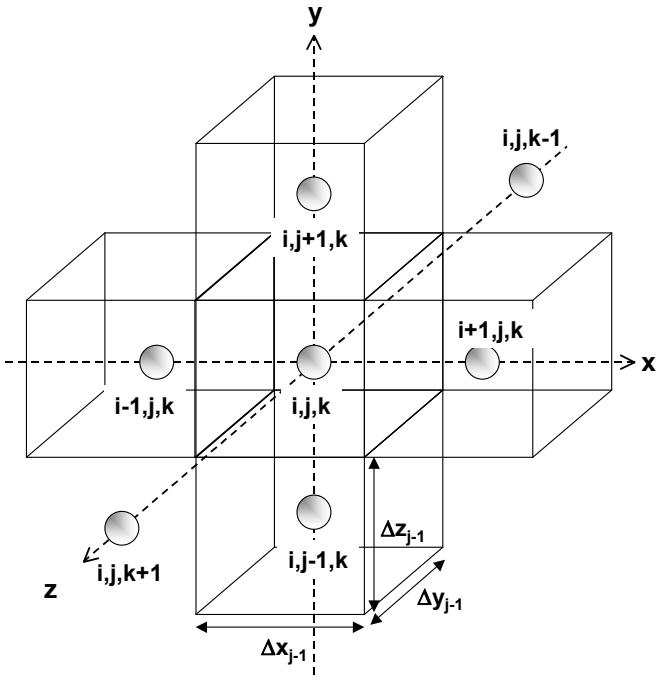

Figure 2.1 Three-dimensional node and cell structure.

At the p+1 th time step, let $\hat{E}^{p+1}_{(i,j,k)}$ be the *rate* of thermal energy accumulated and stored in the (i,j,k)th cell and $\ddot{E}^{p+1}_{(i,j,k)}$ be the *rate* of thermal energy entering and leaving the cell due to temperature across the surface from neighbouring cells. For the (i,j,k)th cell at the p+1th time step, the conservation of energy may be written (corresponding to the form (2.3)) as

$$\hat{E}^{p+1}_{(i,j,k)} = \ddot{E}^{p+1}_{(i,j,k)} . \tag{2.10}$$

In (2.10), the energy transfer rate *into* the (i,j,k)th cell from the surrounding cells (Figure 2.1) is obtained using (2.9) so that

$$\begin{aligned} \ddot{E}^{p+1}_{(i,j,k)} = &\left(q^{p+1}_{(i-1,j,k)\rightarrow(i,j,k)} + q^{p+1}_{(i,j,k)\leftarrow(i+1,j,k)}\right)\Delta y\,\Delta z + \\ &\left(q^{p+1}_{(i,j-1,k)\uparrow(i,j,k)} + q^{p+1}_{(i,j,k)\downarrow(i,j+1,k)}\right)\Delta x\,\Delta z + \\ &\left(q^{p+1}_{(i,j,k-1)\bullet(i,j,k)} + q^{p+1}_{(i,j,k)\otimes(i,j,k+1)}\right)\Delta x\,\Delta y . \end{aligned} \tag{2.11}$$

Using an approach where fluxes from neighbouring cells are defined in a direction into the (i,j,k)th cell is useful as it enables a reduction of the number of different equation forms needed for computation analysis. The rate of change of energy stored in the control volume is simply (see (2.5))

$$\hat{E}^{p+1}_{(i,j,k)} = \frac{\partial}{\partial t}\left(\rho c_v T\right)\Delta x\Delta y\Delta z . \tag{2.12}$$

For a small time step Δt the thermal properties ρ and c_v are assumed to be constant, so the time differential of the temperature in (2.12) can be approximated using finite differences, such that

$$\hat{E}^{p+1}_{(i,j,k)} \cong \rho c_v \frac{\left(T^{p+1}_{(i,j,k)} - T^{p}_{(i,j,k)}\right)}{\Delta t^{p+1}}\Delta x\Delta y\Delta z . \tag{2.13}$$

Inserting (2.13) into (2.10) and rearranging gives a finite difference representation of the temperature at a time period p+1

$$T^{p+1}_{(i,j,k)} = T^{p}_{(i,j,k)} + \frac{1}{\rho c_v}\left(\frac{\Delta t^{p+1}}{\Delta x\Delta y\Delta z}\right)\ddot{E}^{p+1}_{(i,j,k)} , \tag{2.14}$$

where $\ddot{E}^{p+1}_{(i,j,k)}$ is calculated using (2.11) from the temperatures of neighbouring cells, each of which must be derived taking account of the type of surrounding node.

2.3 HEAT FLUXES AT THE MATERIAL CELL INTERFACE

In this model, material cells are defined as cells that contain a homogeneous material for temperature to flow through. The nodes at the centre of these cells are referred to as material nodes. The boundary between two adjacent cells is referred to as a material cell interface. Heat fluxes at the interface of material cells can be estimated using Fourier's law where the flux between the material cells is proportional to the gradient between the temperatures. For a multi-material system where neighbouring material cells could have different properties, an effective thermal conductivity is to be calculated to ensure continuity of the heat fluxes at the cell interfaces.

It is assumed that the $(i,j,k)^{th}$ cell has different thermal conductivity rates along the different principal axes x, y and z. Assume that thermal conductivity is uniform within each of the cell volumes and let the superscripts x, y and z represent cell conductivities in the x, y and z planes respectively. Continuity of flux across the interface between the $(i,j,k)^{th}$ cell and the $(i+1,j,k)^{th}$ cell requires the following equations to be satisfied

$$\lambda_{(i,j,k)|(i+1,j,k)} \frac{\left(T_{(i+1,j,k)} - T_{(i,j,k)}\right)}{\Delta x_{(i+1,j,k)} + \Delta x_{(i,j,k)}} = \lambda^{x}_{(i+1,j,k)} \frac{\left(T_{(i+1,j,k)} - T_{(i,j,k)|(i+1,j,k)}\right)}{\Delta x_{(i+1,j,k)}}, \tag{2.15}$$

$$\lambda_{(i,j,k)|(i+1,j,k)} \frac{\left(T_{(i+1,j,k)} - T_{(i,j,k)}\right)}{\Delta x_{(i+1,j,k)} + \Delta x_{(i,j,k)}} = \lambda^{x}_{(i,j,k)} \frac{\left(T_{(i,j,k)|(i+1,j,k)} - T_{(i,j,k)}\right)}{\Delta x_{(i,j,k)}}, \tag{2.16}$$

where $\lambda_{(i,j,k)|(i+1,j,k)}$ and $T_{(i,j,k)|(i+1,j,k)}$ are the effective thermal conductivity and temperature at the interface between the $(i,j,k)^{th}$ and $(i+1,j,k)^{th}$ cells as shown in Figure 2.2.

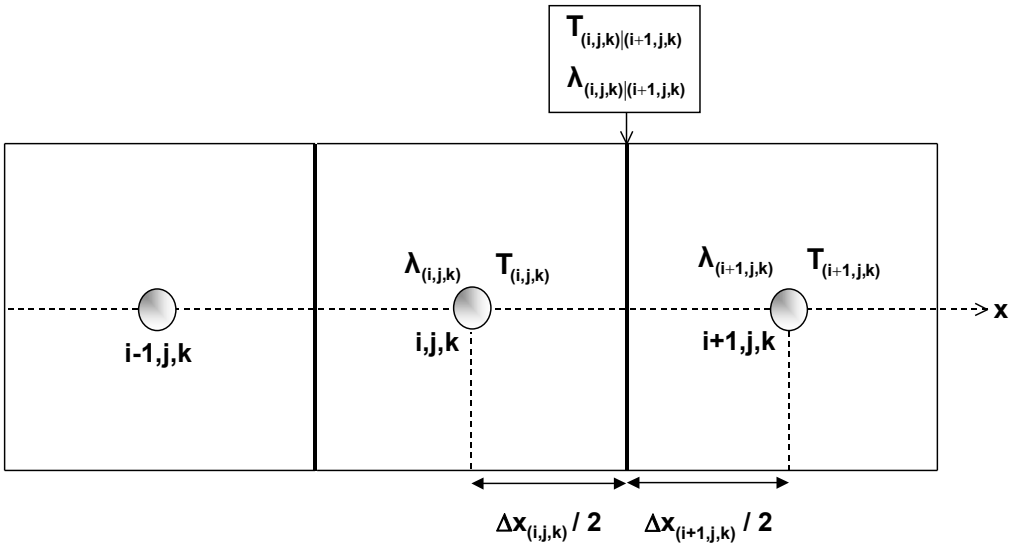

Figure 2.2: The effective thermal conductivity and temperature at the interface between the (i,j,k^{th}) and $(i+1,j,k^{th})$ cells

Eliminating $T_{(i,j,k)|(i+1,j,k)}$ from (2.15) and (2.16), and making $\lambda_{(i,j,k)|(i+1,j,k)}$ the subject of the equations leads to the result

$$\lambda_{(i,j,k)|(i+1,j,k)} = \frac{\lambda^{x}_{(i,j,k)}\,\lambda^{x}_{(i+1,j,k)}\,(\Delta x_{(i+1,j,k)} + \Delta x_{(i,j,k)})}{\lambda^{x}_{(i,j,k)}\,\Delta x_{(i+1,j,k)} + \lambda^{x}_{(i+1,j,k)}\Delta x_{(i,j,k)}} = \lambda_{(i+1,j,k)|(i,j,k)}\,. \tag{2.17}$$

In general for a solid cell that is completely surrounded by solid cells of different material diffusivities (Figure 2.1), the thermal conductivities are

$$\lambda_{(i,j,k)|(i\pm1,j,k)} = \frac{\lambda^{x}_{(i,j,k)}\,\lambda^{x}_{(i\pm1,j,k)}\,(\Delta x_{(i\pm1,j,k)} + \Delta x_{(i,j,k)})}{\lambda^{x}_{(i,j,k)}\,\Delta x_{(i\pm1,j,k)} + \lambda^{x}_{(i\pm1,j,k)}\Delta x_{(i,j,k)}}, \tag{2.18}$$

$$\lambda_{(i,j,k)|(i,j\pm1,k)} = \frac{\lambda^{y}_{(i,j,k)}\,\lambda^{y}_{(i,j\pm1,k)}\,(\Delta y_{(i,j\pm1,k)} + \Delta y_{(i,j,k)})}{\lambda^{y}_{(i,j,k)}\,\Delta y_{(i,j\pm1,k)} + \lambda^{y}_{(i,j\pm1,k)}\Delta y_{(i,j,k)}}, \tag{2.19}$$

$$\lambda_{(i,j,k)|(i,j,k\pm1)} = \frac{\lambda^{z}_{(i,j,k)}\,\lambda^{z}_{(i,j,k\pm1)}\,(\Delta z_{(i,j,k\pm1)} + \Delta z_{(i,j,k)})}{\lambda^{z}_{(i,j,k)}\,\Delta z_{(i,j,k\pm1)} + \lambda^{z}_{(i,j,k\pm1)}\Delta z_{(i,j,k)}}. \tag{2.20}$$

It should be noted that if neighbouring cells have the same value of thermal conductivity (as would be the case if they were material constants), then $\lambda_{(i,j,k)|(i\pm1,j,k)} = \lambda^{x}$ where λ^{x} is the common value. Also, when a cell is located at an external boundary, the correct thermal conductivity arises from (2.18-2.20) if the neighbouring (fictitious) cell is taken to have a zero thickness. Cells of zero thickness do in fact offer a convenient method of imposing a fixed temperature at external boundaries. Such cells partake in the incremental process of advancing time, but their temperature values are not updated.

The fluxes *into* the $(i,j,k)^{th}$ cell from the surrounding cells, for the $p+1^{th}$ time step, can be simply approximated using Fourier's law to give

$$q^{p+1}_{(i-1,j,k)\rightarrow(i,j,k)} = \lambda_{(i,j,k)|(i-1,j,k)}\,\frac{2\left(T^{p}_{(i-1,j,k)} - T^{p}_{(i,j,k)}\right)}{\Delta x_{(i,j,k)} + \Delta x_{(i-1,j,k)}}, \tag{2.21}$$

$$q^{p+1}_{(i,j,k)\leftarrow(i+1,j,k)} = \lambda_{(i,j,k)|(i+1,j,k)}\,\frac{2\left(T^{p}_{(i+1,j,k)} - T^{p}_{(i,j,k)}\right)}{\Delta x_{(i,j,k)} + \Delta x_{(i+1,j,k)}}, \tag{2.22}$$

$$q^{p+1}_{(i,j-1,k)\uparrow(i,j,k)} = \lambda_{(i,j,k)|(i,j-1,k)}\,\frac{2\left(T^{p}_{(i,j-1,k)} - T^{p}_{(i,j,k)}\right)}{\Delta y_{(i,j,k)} + \Delta y_{(i,j-1,k)}}, \tag{2.23}$$

$$q^{p+1}_{(i,j,k)\downarrow(i,j+1,k)} = \lambda_{(i,j,k)|(i,j+1,k)}\,\frac{2\left(T^{p}_{(i,j+1,k)} - T^{p}_{(i,j,k)}\right)}{\Delta x_{(i,j,k)} + \Delta x_{(i,j+1,k)}}, \tag{2.24}$$

$$q^{p+1}_{(i,j,k-1)\bullet(i,j,k)} = \lambda_{(i,j,k)|(i,j,k-1)}\,\frac{2\left(T^{p}_{(i,j,k-1)} - T^{p}_{(i,j,k)}\right)}{\Delta z_{(i,j,k)} + \Delta z_{(i,j,k-1)}}. \tag{2.25}$$

$$q^{p+1}_{(i,j,k)\otimes(i,j,k+1)} = \lambda_{(i,j,k)|(i,j,k+1)} \frac{2\left(T^{p}_{(i,j,k+1)} - T^{p}_{(i,j,k)}\right)}{\Delta x_{(i,j,k)} + \Delta x_{(i,j,k+1)}}. \qquad (2.26)$$

The fluxes in (2.21-2.26) are inserted into (2.11) to calculate the energy transfer rate *into* the $(i,j,k)^{th}$ cell. The advantage of this definition is that all temperature gradients are now of the same form, which is useful when designing efficient algorithms for computational analysis. The temperature over time may then be calculated in an incremental fashion using (2.14).

2.4 HEAT FLUXES AT THE MATERIAL CELL BOUNDARY

When using the relations (2.11) and (2.14) to update the temperature distribution during its evolution, it is necessary to estimate the fluxes at the external boundary where a fixed temperature value has been imposed as a boundary condition. Boundary nodes, that can be associated with the nodes of additional boundary cells having zero thickness, are used to describe *fixed temperature* boundary conditions at the edge or boundary of a material cell. Values of temperatures at the boundary nodes, whose values are denoted by tilde, are used to calculate the temperature of a material cell in the vicinity of a boundary. It is useful to deal with boundary conditions of this type by considering a system having a single cell, so that all its boundaries are external surfaces at which a fixed temperature is imposed, as shown in Figure 2.3. The relations that will be derived from the single cell model will apply also to systems of interest that have many cells on a grid.

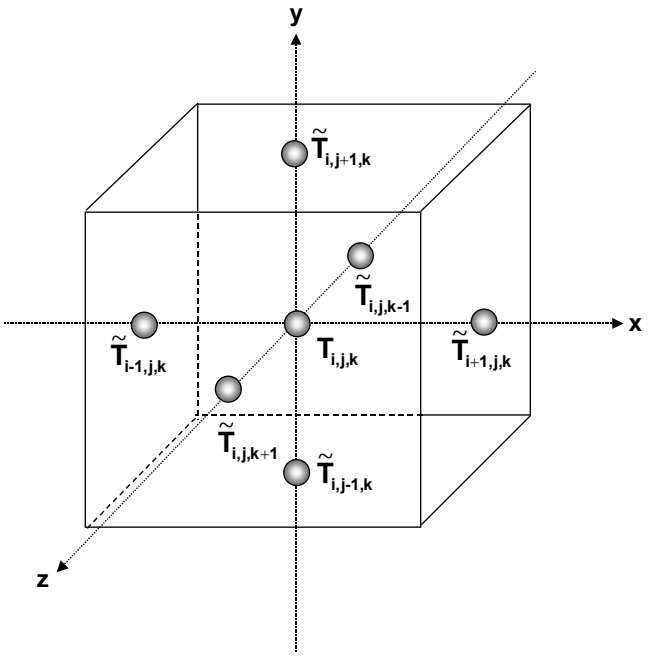

Figure 2.3 Temperatures at the boundaries of the i,j,k^{th} cell

Consider the material cell (i,j,k) with temperature $T^{p}_{(i,j,k)}$ at time p in the absence of surrounding material cells. The boundaries are the edges of the cell and are set as *fixed temperature* boundary conditions with temperatures $\tilde{T}^{p}_{(i+1,j,k)}$, $\tilde{T}^{p}_{(i-1,j,k)}$, $\tilde{T}^{p}_{(i,j+1,k)}$, $\tilde{T}^{p}_{(i,j-1,k)}$, $\tilde{T}^{p}_{(i,j,k+1)}$ and $\tilde{T}^{p}_{(i,j,k-1)}$, as shown in Figure 2.3. The effective heat fluxes from the boundaries are simply

$$q^{p+1}_{(i-1,j,k)\rightarrow(i,j,k)} = \lambda^{x}_{(i,j,k)} \frac{2\left(\tilde{T}^{p}_{(i-1,j,k)} - T^{p}_{(i,j,k)}\right)}{\Delta x_{(i,j,k)}}, \tag{2.27}$$

$$q^{p+1}_{(i,j,k)\leftarrow(i+1,j,k)} = \lambda^{x}_{(i,j,k)} \frac{2\left(\tilde{T}^{p}_{(i+1,j,k)} - T^{p}_{(i,j,k)}\right)}{\Delta x_{(i,j,k)}}, \tag{2.28}$$

$$q^{p+1}_{(i,j-1,k)\uparrow(i,j,k)} = \lambda^{y}_{(i,j,k)} \frac{2\left(\tilde{T}^{p}_{(i,j-1,k)} - T^{p}_{(i,j,k)}\right)}{\Delta y_{(i,j,k)}}, \tag{2.29}$$

$$q^{p+1}_{(i,j,k)\downarrow(i,j+1,k)} = \lambda^{y}_{(i,j,k)} \frac{2\left(\tilde{T}^{p}_{(i,j+1,k)} - T^{p}_{(i,j,k)}\right)}{\Delta y_{(i,j,k)}}, \tag{2.30}$$

$$q^{p+1}_{(i,j,k-1)\bullet(i,j,k)} = \lambda^{z}_{(i,j,k)} \frac{2\left(\tilde{T}^{p}_{(i,j,k-1)} - T^{p}_{(i,j,k)}\right)}{\Delta z_{(i,j,k)}}, \tag{2.31}$$

$$q^{p+1}_{(i,j,k)\otimes(i,j,k+1)} = \lambda^{z}_{(i,j,k)} \frac{2\left(\tilde{T}^{p}_{(i,j,k+1)} - T^{p}_{(i,j,k)}\right)}{\Delta z_{(i,j,k)}}. \tag{2.32}$$

The results (2.27-2.32) apply also at the external cells of a system having multiple cells. When a boundary is encountered, the heat fluxes in (2.27-2.32) are inserted into (2.11), as before, and the temperature over time may then be calculated in an incremental fashion using (2.14), together with values generated by the initial temperature distribution (usually uniform throughout the system). When considering updating the temperatures of internal cells, the relations (2.21-2.26) involving effective thermal conductivities are used. It should be noted that the expressions in (2.27-2.32) can be obtained from (2.21-2.26) by setting the cells surrounding the $(i,j,k)^{th}$ to have zero cell size.

Transient solutions for the temperature at the $(i,j,k)^{th}$ cell can easily be constructed by using the appropriate equation for the heat fluxes depending on whether the edge of the cell is an interface with another material cell (2.21-2.26) or a boundary with a fixed temperature (2.27-2.32). When applying a *fixed heat flux* at the boundaries, the values for the imposed flux are substituted directly into (2.11) at the appropriate boundary.

3 MODIFICATION OF THE THEORY FOR COUPLING WITH MTDATA

In this section a method is described to link the software packages TherMOL 3D and MTDATA in order to model the relationship between the temperature of a cell at a given instant in time and the stored energy at a given pressure.

3.1 MODIFICATION OF THE ENERGY BALANCE EQUATIONS FOR USE WITH MTDATA

The TherMOL 3D software is a heat transfer tool for use with 3-D multi-material systems based on the theory outlined in section 2. A simple modification to the energy balance equations used by

TherMOL 3D is described here to enable a fundamental link with the thermodynamic phase equilibria package MTDATA.

The *change* of thermal energy accumulated and stored in the $(i,j,k)^{th}$ cell over a time period Δt is defined as $\Delta E_{(i,j,k)}$. Using the conservation of energy for small time periods, we may write

$$\frac{\Delta E_{(i,j,k)}}{\Delta t} = \ddot{E}_{(i,j,k)} \ , \tag{3.1}$$

where $\ddot{E}_{(i,j,k)}$ is the *rate* of thermal energy entering and leaving the cell due to temperature across the surface from neighbouring cells during the time period Δt. Integrating (3.1) and rearranging gives a simple representation of energy at the $p+1^{th}$ time step

$$E^{p+1}_{(i,j,k)} = E^{p}_{(i,j,k)} + \ddot{E}^{p+1}_{(i,j,k)} \, \Delta t \ , \tag{3.2}$$

where $\ddot{E}^{p+1}_{(i,j,k)}$ is calculated from (2.11) using the heat fluxes, each of which must be derived depending on the type of the surrounding node, as described in Section 2. The temperatures for each cell at each time step are calculated from the stored energy by MTDATA and this is described in more detail in the next section.

3.2 RELATIONSHIP BETWEEN STORED ENERGY AND TEMPERATURE

MTDATA can be used to calculate phase and chemical equilibria for multi-component systems containing many different types of phase. MTDATA has the capability to perform calculations for as many as 30 different components with up to 500 phases being considered at the same time. Included in the software is a range of models that describe the thermodynamic properties for different types of phase as a function of temperature, pressure and composition, and a number of databases are available containing critically assessed thermodynamic data for various types of material. The principles of the calculation of chemical and phase equilibria are well established and are described in the review by Bale 1990.

Let the number of species and components in a system be given by N and M respectively, where distinct chemical species are formed from one of more chemical components within a particular phase such that $M \le N$. If we define ν_n as the number of moles of species n present in the system and μ_n as the chemical potential of the n^{th} species, then the equilibrium state of a system at a given temperature and pressure may be determined by minimising the Gibbs energy function G, given by

$$G = \sum_{n=1}^{N} \nu_n \mu_n \qquad n = 1, 2 \ldots N \ , \tag{3.3}$$

subject to M composition constraints

$$\sum_{n=1}^{N} a_{mn} \nu_n = r_m \qquad n = 1, 2 \ldots N \ , \ m = 1, 2 \ldots M \ , \tag{3.4}$$

where a_{mn} is the number of units of component m per species n and r_m is the number of moles of component m in the system. It should be noted that μ_n may be a function of some or all of the species

amounts in the same phase and is also dependent on temperature and pressure. The expression G is a non-linear function of the species amounts and is dependent on temperature, composition and pressure. The minimisation of G is accomplished by varying ν_n and this is done in MTDATA using a robust true Gibbs energy minimisation procedure based on the NPL developed NOSL (Numerical Optimisation Software Library) library (Gill *et al* 1981).

Given the composition, temperature and pressure of the system, MTDATA will calculate the Gibbs energy and equilibrium state in terms of the distribution of components and species between the stable phases. The stored energy E (enthalpy) can then be calculated from the Gibbs energy for a temperature T by using the relation

$$E = \frac{\partial\left(G/T\right)}{\partial\left(1/T\right)}, \tag{3.5}$$

which can be derived directly from the laws of thermodynamics (Hillert *et al* 1998) for conditions of fixed pressure and composition. The stored energy can also be applied as a constraint to this optimisation allowing temperature to be determined for a given stored energy. For linking with TherMOL 3D, MTDATA is initially used to calculate the energy stored in each cell at a given pressure from the initial temperatures of the cells. Incrementing in time Δt, TherMOL 3D then calculates the fluxes across all the cells due to the applied boundary conditions, and so the new energy stored in each cell at the end of the time step is calculated. MTDATA is then used to calculate the new cell temperature from the stored energy.

It should be noted that as MTDATA calculates the Gibbs energy for the complete multi-phase system, the change in heat capacity with temperature and any complex variations in heat capacity due to phase changes are implicitly accounted for. In addition to equilibrium calculations it is possible to simulate non-equilibrium conditions by omitting phases. This can be important in the type of simulation described in this report as it can be necessary to suppress the formation of certain phases until specific conditions are reached.

4 RESULTS AND DISCUSSION

The NPL materials modelling framework was used to code the heat-diffusion software TherMOL 3D and link with the MTDATA software (using a DLL). The modelling framework uses the Java programming language and is fully object-oriented adopting XML and MatML for data handling. This section describes results obtained from both the hybrid and TherMOL 3D models for a steel block subjected to a heat flux boundary condition.

4.1 MODEL SETUP AND DATA

A simple case of a steel block subjected to a uniform, time independent heat flux boundary condition on one surface was studied. The MTDATA calculations used were all for a steel with composition Fe – 0.5 mass% C – 5 mass% Cr and the thermodynamic data was taken from the NPL MTSOL database. To improve the speed of the calculations, phases that would not form for this composition at the temperature range considered were not included. The phases considered were BCC_A2 (ferrite), FCC_A1 (austenite), M7C3 and Liquid alloy.

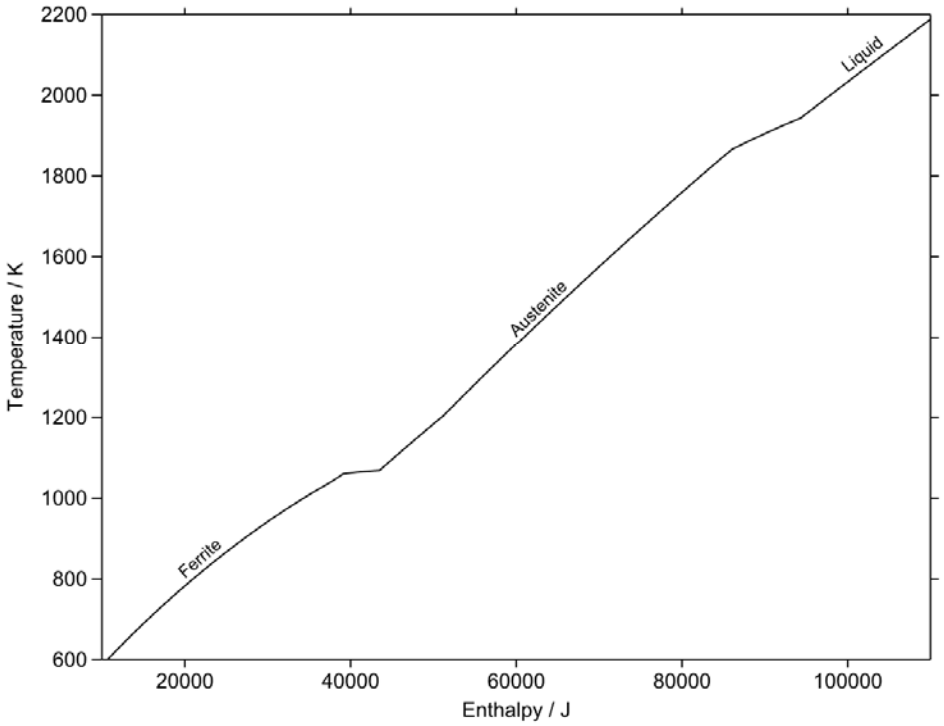

Figure 4.1 Enthalpy vs temperature plot for Fe-0.5%C-5%Cr steel alloy calculated directly by MTDATA.

Figure 4.1 shows a plot of temperature against enthalpy for the steel alloy as calculated directly by MTDATA. It can be seen that there are two clear phase changes indicated by sharp changes in gradient of the line. The phase changes are ferrite to austenite at approximately 1060 K and austenite to liquid starting at approximately 1860 K. There is also another small effect at approximately 1200 K, which is the temperature at which the M7C3 phase disappears on heating, but otherwise there are no other thermal effects. The austenite and liquid regions are approximately linear, however the non-linearity in the ferrite region is due to a gradual increase in the heat capacity as the ferrite phase heats up.

All the TherMOL 3D grid geometries described in the following sections were for a block with dimensions 1 cm x 1 cm x 10 cm, and were modelled using a stack of 3-D cells of various numbers in the 10 cm direction. A heat flux boundary condition was imposed on the top surface (i.e. 1 cm x 1 cm) of the block, with the remaining 5 surfaces having thermally insulated conditions. The mass of each cell was needed to set the composition in MTDATA and this was determined from the cell volume using a value of 7770 kg/m^3 for the density. A constant value of 30.86 W/(m^2·K) was used for the thermal conductivity of the material for all runs. For runs that did not call MTDATA (TherMOL 3D only) a fixed value of 495 J/(kg·K) was used for the heat capacity at constant pressure of the material, as this was the heat capacity calculated by MTDATA for this material at 400 K.

The maximum stable time step for each run was found by trial and error. If the time step was too large the run would become unstable and a smaller time step was used. For smaller grid sizes, smaller time steps were necessary for stability. TherMOL 3D also uses a fixed grid with each cell being a constant volume, however the MTDATA calculations are for fixed pressure conditions and use enthalpy to represent the stored energy in TherMOL 3D. To properly match TherMOL 3D, the thermodynamic calculations should be performed at a fixed volume and use internal energy rather than enthalpy. For the cases considered in this report, the difference between the internal energy and enthalpy for condensed phases at low to moderate pressures is not significant (Dinsdale 1991).

4.2 FIXED HEAT FLUX BOUNDARY CONDITION RESULTS

This study used a grid size of 10 cells where each cell was a 1 cm cube. At the start of the run each cell was set at a temperature of 400 K. The imposed boundary condition was a fixed heat flux of 1.2 MW/m^2 applied to the top surface of the grid. The other surfaces have a thermally insulated boundary condition and the run started with each cell at a temperature of 400 K.

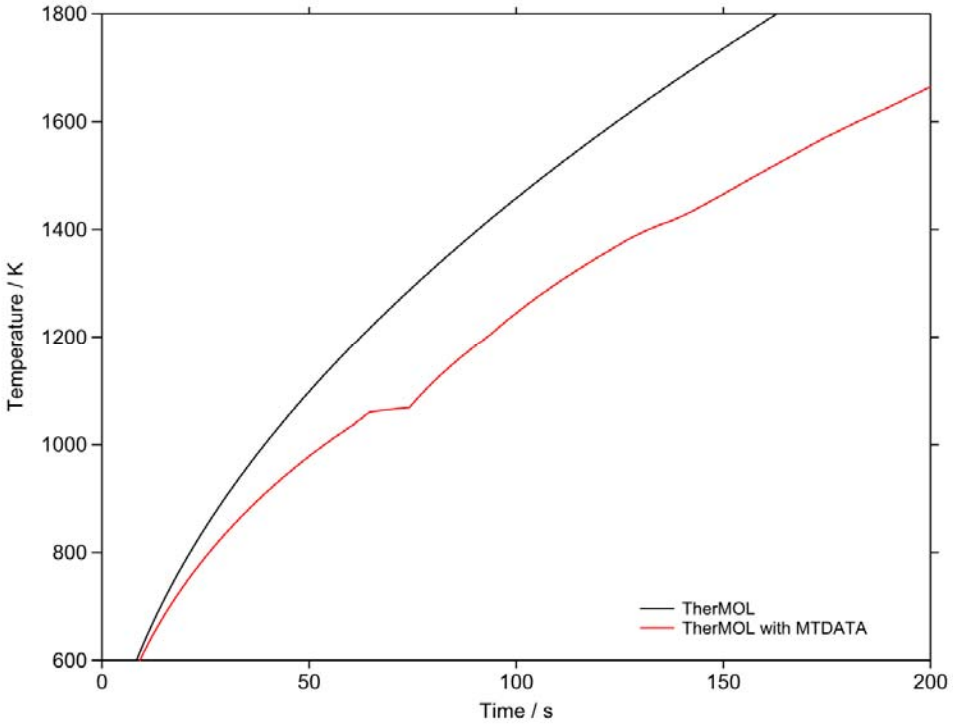

Figure 4.2 Temperature of the top surface cell for original TherMOL and TherMOL calling MTDATA, with a fixed heat flux boundary condition and a grid size of 10 cells.

The result of the fixed heat flux boundary condition runs are shown in Figure 4.2 and a comparison is made with a run from the original TherMOL 3D. Figure 4.2 shows an increasing difference in temperature between the two runs as time proceeds. This is because the heat input into the system is the same in both cases, but in the run calling MTDATA, the heat capacity of the material is increasing with temperature, changing from 495 J/(kg·K) at 400 K to 1017 J/(kg·K) at 1000 K.

The hybrid model shows a slight change in the temperature-time curve that can be seen at a temperature above the ferrite to austenite phase transition. The change in the curve occurs at a temperature of about 1400 K. There is no equilibrium thermal effect at this temperature as can be seen in Figure 4.1. The effect seen with the hybrid model is a result of modelling the heat flow using a coarse grid as the temperature of the cell is being affected by equilibrium phase changes in neighbouring cells.

Figure 4.3 shows temperature-time curves of the top surface cell and cells 1 cm and 2 cm into the grid for the fixed heat flux run. The curves show the full temperature/time curves up to 500 s and it is clearly seen that a phase transition in one cell is causing thermal effects in the neighbouring cells.

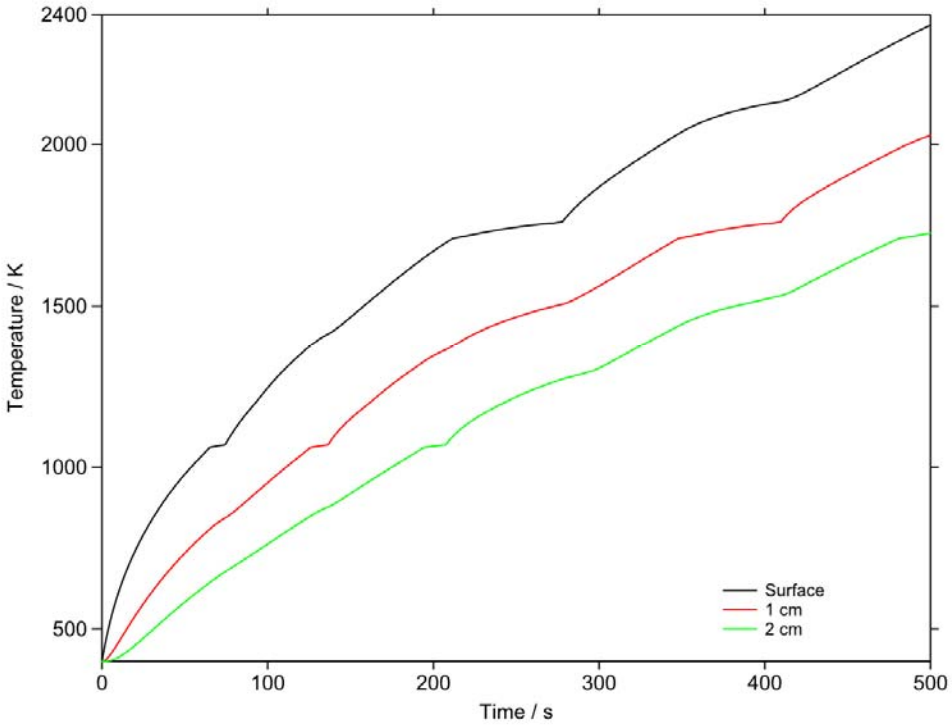

Figure 4.3 Temperatures of the top surface cell, 1 cm deep and 2 cm deep cells for the hybrid model with a fixed heat flux boundary condition and a grid size of 10 cells.

Using numerical methods based on discretising the material, the sharp effects due to phase transition in neighbouring cells will occur. In reality the sharpness of the effect on the temperature/time curve should be smoothed out over a large temperature range rather than occurring at a certain time. To investigate this suggestion a run was carried out using a finer grid. Figure 4.4 shows the result from a run with a grid size of 20 cells, with each cell having a size of 1 cm x 1 cm x 0.5 cm, giving the same overall size for the block.

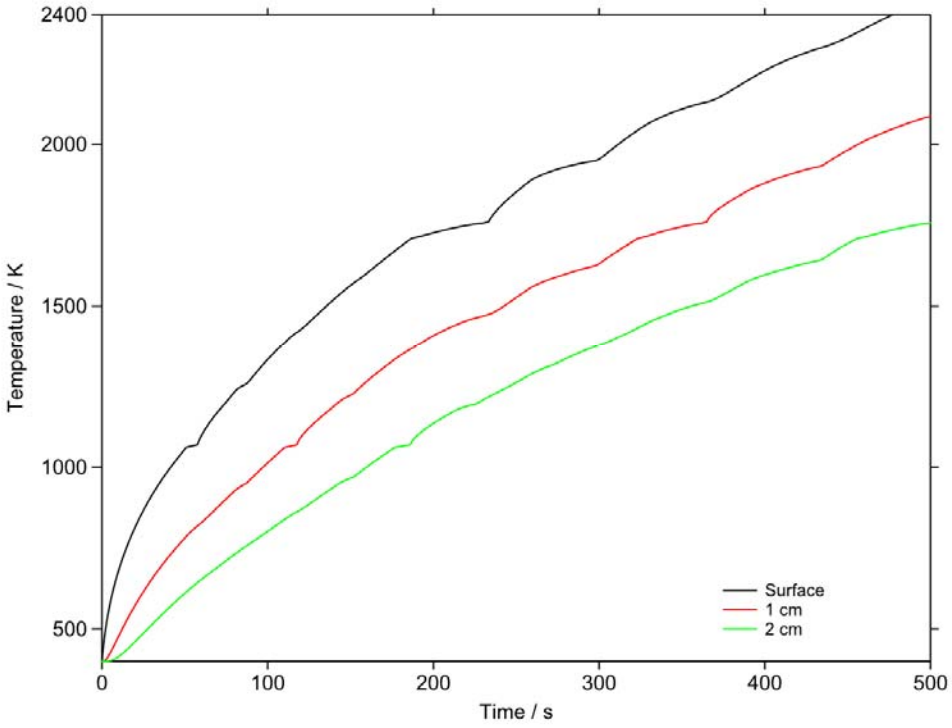

Figure 4.4 Temperatures of the top surface cell, 1 cm deep and 2 cm deep cells for the hybrid model with a constant heat flux boundary condition and a grid size of 20 cells.

As in the previous runs, the phase transitions can clearly be seen at the same temperatures as before but now there are extra thermal effects, which are smaller in magnitude. There are more of these effects because there are more cells per unit volume in the grid, but as each cell is smaller each effect is reduced. This phenomenon is confirmed in Figure 4.5.

Figure 4.5 shows the top surface cell temperature from 3 different runs, with grid sizes of 10, 20 and 40 cells. This clearly shows the extra thermal effects being smoothed out as the number of cells in the grid increases. Another important feature shown here is that the temperature of the top surface cell appears to rise as the number of cells in the grid increases. This is entirely to be expected, as using a finer grid the cells are smaller but the heat input is the same, so the surface cell, representing a smaller volume, heats up faster. The overall temperature of the block will be similar for all grid sizes and it would be expected that for extremely fine grids the sharp effect from phase changes from neighbouring cells would completely disappear.

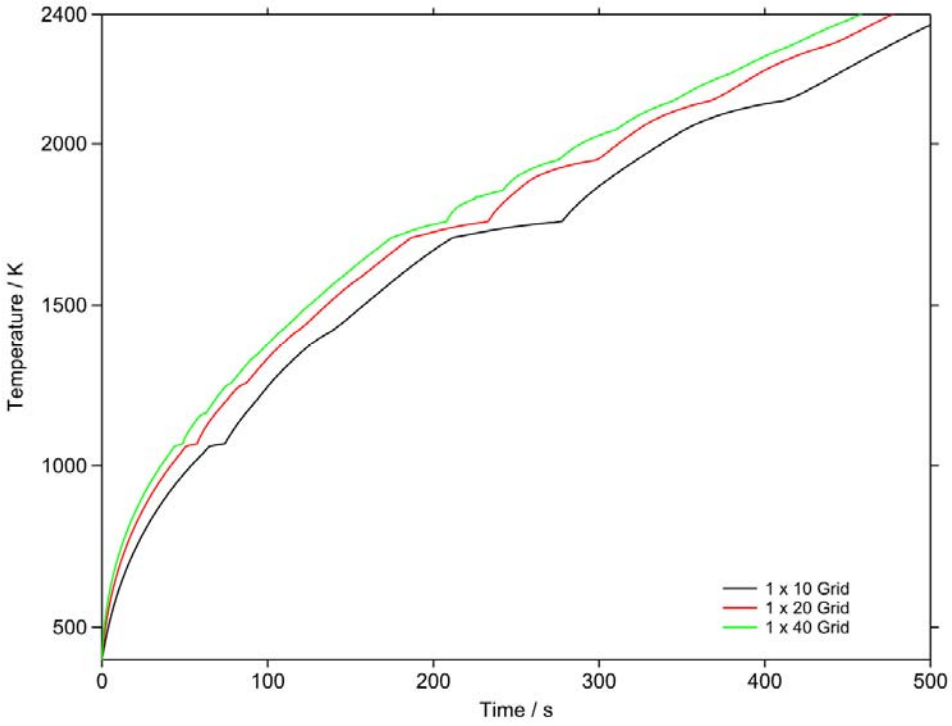

Figure 4.5 Temperature of the top surface cell for hybrid model with a constant heat flux boundary condition for various grid sizes.

The thermal effects caused by neighbouring cells have important implications on the speed of performing these types of calculations. In order to smooth out these effects and realistically model complex material systems with phase changes, finer grids will be necessary and smaller time steps will be needed to maintain stability.

5 FUTURE WORK

When modelling temperature and phase in real life applications, such as casting, the phase changes of the material can lead to significant changes in the geometry of the material. TherMOL 3D currently uses a grid of fixed volume cells where at the start of each simulation the geometry and cell distribution is set and fixed for the duration of the simulation. As a result, the MTDATA calculations used here are performed at fixed pressure and the difference between the thermodynamic calculations performed at fixed pressure and fixed volume was assumed to be insignificant for the purposes of this study. However this may not be the case with other material types, particularly those involving large volume changes with temperature and volume differences between phases. The finite volume method described here could be modified to take account of these volume changes, however the sensible approach would be to use the finite element method. If future TherMOL 3D software adopted a finite element approach, calculating the thermodynamic properties at fixed pressure is possible, allowing the volume-temperature relationship to be calculated by MTDATA as well as the energy-temperature relationship.

In running the hybrid model it was clear that the speed of the MTDATA calls is the most significant factor in the total time of a simulation. To successfully develop the hybrid model further finer grids are required and hence smaller time steps. This would mean that a typical run will take much longer to complete so it is extremely important to optimise the speed of the MTDATA calculations. Obtaining the temperature from a given enthalpy is not a typical way in which MTDATA has been

previously used and so little effort has been put into optimising this method. There are likely to be speed improvements that could be made by improving these algorithms. Modifying the current hybrid software to run on multi-processor hardware would also lead to improvements as shown in similar applications outlined by Esward *et al* 2006 and Meng and Wang 2004.

Another material property that is an important input for TherMOL 3D is thermal conductivity. Currently a constant value is used by TherMOL 3D but this is known to be unrealistic as, like other thermo-physical properties, it will change with temperature and material phase. Models for thermal conductivity for some materials (aluminium alloys in an annealed state and steels) have been developed as part of other DTI sponsored projects (Quested *et al* 2000). A future development should be to investigate the effect of including these models on the output from TherMOL 3D and if significant to develop models for other material types.

6 CONCLUSIONS

From the derivations and results presented in this report the following conclusions may be drawn:

- A mathematical model has been derived to predict the temperature distribution of 3-dimensional, multi-material systems subjected fixed temperature or heat flux boundary conditions that could result in changes of material phase. A novel approach altering the energy balance at a fundamental level has been used to incorporate phase change behaviour into standard heat-conduction theory.

- A numerical solution method has been developed that modifies the standard finite volume methodology (used by TherMOL 3D) to include calculations from the thermodynamic software package MTDATA

- As MTDATA can calculate the relationship between stored energy and temperature for a multi-phase multi-component system, the change in heat capacity with temperature and any complex variations in heat capacity due to phase changes are implicitly accounted for.

- A successful software application linking TherMOL 3D and MTDATA has been developed. The object-oriented Java modelling framework, developed at NPL, has been ideal for developing this hybrid model.

- Comparison of predictions from the hybrid model and the original TherMOL 3D model of a steel block, subjected to heat flux boundary conditions, clearly show the effect of phase change and heat capacity on the temperature distribution.

- It was discovered when running the hybrid model that phase changes affected the temperature rise in neighbouring cells, with the number of these effects increasing but becoming smaller as the grid was refined.

- To realistically model complex material systems using the hybrid model, finer grids will be necessary and smaller time steps will be needed to maintain stability.

7 ACKNOWLEDGEMENTS

The research reported in this report was funded by the UK Department of Trade and Industry (National Measurement System Policy Unit) as part of the Thermal and Materials Metrology Programme (2007 - 2010) and also the NPL Strategic Research Programme.

REFERENCES

Armitt et al, "*The Spalling of Steam-Grown Oxide from Superheater and Reheater Tube Steels*". EPRI report, February 1978.

Bale C. W. and Eriksson G., *Canad. Metal. Quart*., Vol. 29, 105-132, 1990.

Barth, T. and Ohlberger M., *"Finite Volume Methods: Foundation and Analysis"*, Encyclopaedia of Computational Mechanics, John Wiley and Sons, 2004.

Carslaw H. S. and Jaeger J. C., *"Conduction of Heat in Solids"*, Oxford University Press, Second Edition, 1993.

Chapman L. A., "*Application of High Temperature DSC Technique to Nickel Based Superalloys*", J. Mat. Sci., 39(24), pp 7229-7236, 2004.

Chapman L. A., Fry A. T. and Roberts S. J., *"Thermal Diffusivity and Thermal Conductivity Measurements on Oxide Scales"*, NPL Report DEPC-MPE 018, July 2005.

Davies R. H., Dinsdale A. T., Gisby J. A., Robinson J. A. J. and Martin S. M., *"MTDATA – Thermodynamic and Phase Equilibrium Software from the National Physical Laboratory"*, CALPHAD, Vol. 26(2), pp. 229-271, 2002.

Dinsdale A. T., *"SGTE Data for Pure Elements"*, CALPHAD, Vol. 15(4), pp. 317-425, 1991.

Duncan B. C., Pilkington G., Nottay J. S., Allen C. R. G., Lawrence K., Urquhart J and Roberts S. J. *"Diffusion of Moisture in Adhesive Bonds"*, NPL Report DEPC-MPR 062, March 2007

Esward T. J., McCormick N. J., Lawrence K. M. and Stevens M. J., *"Distributed Computing for Metrology Applications"*, SSFM Good Practice guide No. 17, NPL Report DEM-ES 006, March 2006.

Feng Y., Yu B., Zou M and Zhang D, *"A Generalised Model for the Effective Thermal Conductivity of Porous Media Based on Self-Similarity"*, J. Phys. D: Appl. Phys. Vol 37, pp. 3030-3040, 2004.

Fourier, J. B. *"Théorie Analytique de la Chaleur"*(1822), English Translation by A Freeman, Dover Publ., New York, 1955.

Gill P., Murray W. and Wright M., *"Practical Optimisation"*, Academic Press, London 1981.

Hillert M., *"Phase Equilibria, Phase Diagrams and Phase Transformations – Their Thermodynamic Basis"*, Cambridge University Press, 1998.

Hong C, *"Computer Modelling of Heat and Fluid Flow in Materials Processing"*, Institute of Physics Publishing, 2004.

Howse M., *"Aero Gas Turbines - An Ever-changing Engineering Challenge"*, Rolls-Royce plc, Whittle Lecture at Royal Aeronautical Society, London, 2004.

Hsu T. R., *"The Finite Element Method in Thermomechanics"*, Allen & Unwin Inc, 1986.

Incropera F. P. and De Witt D. P., *"Fundamentals of Heat and Mass Transfer"*, John Wiley and Sons, Third Edition, 1981.

Jou D. and Casas-Vazquez J., *"Extended Irreversible Thermodynamics of Heat Conduction"*, Eur. J. Phys., Vol. 9, pp. 329-333, 1988.

Lienhard, J. H., *"A Heat Transfer Handbook"*, Phlogiston Press, Cambridge Massachusetts, Third Edition, 2004.

Meng. H and Wang C Y, *"Large-scale Simulation of Polymer Electrolyte Fuel Cells by Parallel Computing"*. Chemical Engineering Sciences, 59, pp 3331-3343, 2004.

Peiró J. and Sherwin S., *"Finite Difference, Finite Element and Finite Volume Methods for Partial Differential Equations"*, Handbook of Materials Modeling. Volume I: Methods and Models, Springer. pp. 1-32, 2005.

Quested P. N., Dinsdale A. T., Robinson J. A. J., Mills K. C. and Hunt J. D., *"The Prediction of the Thermophysical Properties and the Solidification of Commercial Alloys"*, NPL Report CMMT(A)275, 2000.